Structural probing of clusters and gels of self-aggregated magnetic nanoparticles

Bruno Frka-Petesic, Emmanuelle Dubois, Laszlo Almasy, Vincent Dupuis, Fabrice Cousin, Régine Perzynski

Structural probing of clusters and gels of self-aggregated magnetic nanoparticles

B. Frka-Petesic [1] , *E. Dubois* [1] , *L. Almasy* [1] , *V. Dupuis* [1] , *Fabrice Cousin* [2] , *Régine Perzynski* [1]

[1] *UPMC PECSA UMR 7195 case 51, 4 place Jussieu, 75005 Paris - France,*
[2] *LLB CEA-CNRS UMR 12, CE-Saclay, 91191 Gif-sur-Yvette - France*

The microstructure of home-made aqueous magnetic fluids based on maghemite ($\gamma-Fe_2O_3$) and cobalt ferrite ($CoFe_2O_4$) nanoparticles is monitored from repulsive on average towards attractive on average by tuning the interparticule electrostatic repulsion through modulations of ionic strength and pH. A self-aggregation leading to sols of individual clusters and/or a thixotropic gel phase is induced. Their microstructure in finely controlled physico-chemical conditions is probed in zero field by Small Angle X-ray Scattering and Ultra-Small Angle Neutron Scattering.

Introduction Aqueous magnetic fluids and clusters of their magnetic nanoparticles are used in a number of biological applications and medical issues, such as MRI contrast agents, for magnetic cell labelling or magneto-thermocytolyse [1, 2, 3, 4]. In these magneto-biological applications as well as in more standard technical applications of magnetic fluids, understanding in a predictive way the state of dispersion of the magnetic nanoparticles is of paramount importance. Home-made magnetic nanoparticles, based on iron oxides and stabilized by electrostatic repulsion, are frequently used in such bio-application [5, 6]. The knowledge and the control of the microstructure of their aqueous dispersions is a serious stake [7, 8, 9, 10, 11, 12]. Monitoring synthesis parameters such as ionic strength, pH, NP coating, NP diameter d and volume fraction Φ in these home-made ferrofluids allows to control the under-field microstructure [13, 14, 15]. By tuning the interparticle interaction potential from repulsive on average to attractive on average, a self-aggregation is induced here in a controlled way, leading either to sols of clusters or to thixotropic gels [16]. We probe the microstructure of these colloidal dispersions in the attractive regime, remaining far from irreversible flocculation, by Small Angle X-ray Scattering (SAXS) experiments performed at European Synchrotron Radiation Facility (ESRF) - Grenoble - France and by Small Angle Neutron Scattering (SANS) performed at Lab. Léon Brillouin (LLB) - CEA - Saclay - France.

1. Ferrofluid samples Here we use γ-Fe_2O_3 (maghemite) and $CoFe_2O_4$ nanoparticles (NPs), chemically synthesized and dispersed in acidic aqueous media following the process described in [17, 18]. They are used in their native form, surface coated with hydroxo ligands -OH, thus neutral (and non stabilized) at $pH = 7$ but positively charged (and stabilized) at $pH \sim 2$ to 3. A size sorting process [19] allows to reduce the initial polydispersity in size of the NPs. This process is applied for synthesizing all the samples used here. Physico-chemical characteristics such as pH, ionic strength and osmotic pressure are fixed by osmotic compression [14]. The NP's volume fraction Φ which is here always $\sim 1.5\%$ is determined by chemical titration of iron. The ionic strength I_{ion} is defined as $\frac{1}{2}\sum_i(z_i^2 c_i)$ where z_i

is the valency and c_i the concentration of the i^{th} species in the solution, which are here H^+ and NO_3^- coming from the initial synthesis and TMA^+ and NO_3^- coming from the dialysis bath. It thus leads here to $I_{ion} = [TMA^+] + 10^{-pH}$. As these dilute Magnetic Fluids are paramagnetic materials, a fit of the room temperature magnetization of samples at low ionic strength and $pH = 2$, by a Langevin formalism weighted with a log-normal distribution of diameters [2] allows to deduce the NP size distribution. Table 1 presents for the various samples, the median diameter d_0, the polydispersity σ, the NP material magnetization m_s. The initial susceptibility χ_0 of these samples is experimentally determined and the magnetic dipolar parameter in the dispersion $\gamma = (\mu_0 m_s^2(\pi d^3/6)\Phi)/kT$ is then deduced here from $\gamma = 3\chi_0$. Table 1 presents both the parameter $\Psi_{dd} = \gamma/\Phi$ characteristic of the size distribution of the NPs and the magnetic dipolar parameter at contact $\lambda* = (\gamma/\Phi)/24$, which ranges here from 0.5 to 2.2, a zero-field chaining of the nanoparticles being thus only possible for the largest NPs.

In the dispersions, the interparticle potential contains three contributions

Samples	material	d_0(nm)	σ	m_s (kA/m)	Ψ_{dd}	$\lambda*$
A	$\gamma-Fe_2O_3$	7.6	0.23	295	12	0.5
B	$\gamma-Fe_2O_3$	8.5	0.25	280	22	0.9
C	$\gamma-Fe_2O_3$	10.5	0.30	315	54	2.2
D	$CoFe_2O_4$	7.6	0.21	290	23.5	1.0
E	$CoFe_2O_4$	9.4	0.36	300	53	2.2

Table 1: Magnetic characteristics of the nanoparticles in the probed samples - see text for the definitions.

related to van der Waals attraction (U_{vdw}), electrostatic repulsion (U_{elec}) and dipole-dipole magnetic interaction (U_{dd}) which is attractive on average in zero field. Each of these contributions can be here modulated by the various experimental parameters : U_{vdw} by the nature of the magnetic material of NPs [8], the intensity of U_{elec} through pH variations and its range through I_{ion} [20, 21, 22] and U_{dd} through the NP size distribution [10, 12].

2. Experimental phase diagram In a previous work [16], a phase diagram of similar samples at different Φ's and based on the same maghemite NPs in the whole range of pH has been built up (see Fig. 1-left). Let us first underline that such samples evolve after their preparation and can be studied at different ages. In [16], samples older than six months and no longer evolving were studied. It has been shown there that between the two sol phases at low and high pH and the flocculation area around $pH = 7$, a thin area exists where the system behaves as a thixotropic gel, solid at rest and flowing when gently shaked. In [16], the ionic strength was not precisely adjusted. Here we compare samples of different size distributions and based on different magnetic materials, at equivalent volume fractions, in the same range as in Fig. 1-left, with both ionic strength I_{ion} and pH tuned by osmotic compression [23]. The results are presented for the freshly prepared samples, as just extracted from their dialysis bag and the evolution with time of this phase diagram [24] will be discussed elsewhere. This diagram I_{ion} versus pH, as determined by our macroscopic observations (Fig. 1-right), is clearly separated in two areas, one situated bottom-left where we observe spontaneously flowing samples, named sol in the diagram and a second one upper-right where

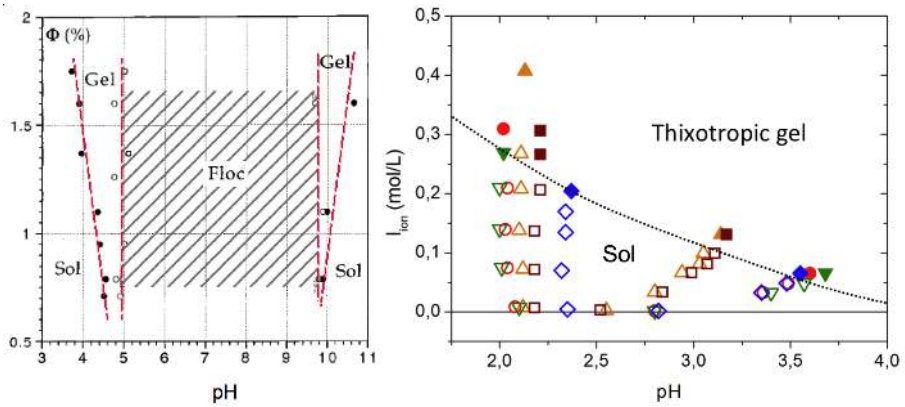

Figure 1: (left part) - Phase diagram obtained in [16] with a maghemite sample (d_0 = 7.1 nm, $\sigma = 0.4$) at $I_{ion} \sim 0.05$ mol/L and t_w more than 6 months; (right part) - I_{ion} as a function of pH for all the samples of Table 1 at $\Phi \sim 1.5\%$, open symbols (samples A to E : $\triangle$, $\circ$, $\square$, $\triangledown$, $\diamond$) correspond to sols and associated closed symbols to gels, as determined by macroscopic observation on samples freshly extracted from their dialysis bag ($t_w = 0$).

the sample is a thixotropic gel. The limit between these two areas depends neither on the size distribution of the NPs nor on the material, on which they are based. However we have observed that this limit is moving downwards in the diagram as time is passing. Indeed as already said, ageing occurs in these systems and some samples undergo a sol-gel transition. As an example, the gel limit at $pH = 2$ which is at $I_{ion} = 0.27 \pm 0.03$ mol/L in samples freshly extracted from their dialysis bag shifts to $I_{ion} = 0.12 \pm 0.03$ mol/L after a time $t_w = 41$ days (t_w is called further on the age of the sample).

To fill up an experimental cell with a thixotropic gel, it is necessary to shake the gel. This shaking process breaks the weak solid structure of the material to be probed. The "shaken gel" is a flowing material which afterwards undergoes in the cell another sol-gel transition (in a much shorter time) leading to the "regenerated gel" which is anew a soft solid. This second sol-gel transition has been already studied in [16, 25, 26] by relaxation of magneto-birefringence and by mechanical spectroscopy, for similar samples as those of Fig. 1-left.

3. Small Angle Scattering experiments To probe the structure of these systems we perform Small Angle X-ray Scattering experiments at the ID02 beamline of ESRF- Grenoble using an energy of 12 keV in the q-range 8 10^{-4} (or 1.5 10^{-3}) Å^{-1} to 0.3 Å^{-1}. The samples are put in flat cells of thickness 1 mm with mica windows. To extend the probing of the micro-structure at lower q's values, a Ultra-Small Angle Neutron Scattering experiment is performed at TPA spectrometer of LLB - Saclay down to $q = 4\ 10^{-4}$ Å^{-1} with a calibration at larger angle on PAXY. The solvent being H_2O, the magnetic scattering coming from the NPs is here negligible and the scattered signal is dominantly of nuclear origin [27].

The scattered patterns being isotropic, the scattered intensity at a given couple (I_{ion}, pH) $I(q, \Phi)$ is radially averaged along rings at constant q and can be written as :

$$I(q,\Phi) \propto \Phi F(q) S(q,\Phi) \tag{1}$$

where $F(q)$ and $S(q,\Phi)$ are the form factor and the static structure factor of the nanoparticles respectively. In order to determine the form factor $F(q)$, a scattering experiment is performed, for each kind of nanoparticles, in a non-interacting situation for which $S(q) = 1$. The structure factor is then obtained, for each couple (I_{ion}, pH), using :

$$S(q,\Phi) = \frac{\Phi_{\mathrm{nonInt}} I(q,\Phi)}{\Phi I_{\mathrm{nonInt}}(q,\Phi_{\mathrm{nonInt}})}. \tag{2}$$

In the experiment, the interparticle interaction evolves from repulsive on average to attractive on average. Repulsive regimes, have been extensively studied in previous studies [13, 14, 15, 28, 29], the structure factor presents then a maximum at the mean interparticle distance and a pronounced decrease at low q's associated to the weak compressibility of the system. In attractive regimes, the particles usually aggregate together to form clusters. If there is no inter-cluster interaction the low q's part of the structure factor can be identified to the form factor of the clusters [30, 31, 32], giving then reliable informations on structure, shape, mean size and number of aggregation of the clusters N_{agg} :

$$N_{agg} = \lim_{q \to 0} S(q). \tag{3}$$

4. Experimental results and discussion We separate this part in two subsections, examing first the results obtained for all the samples of Table 1 when they are freshly extracted from their dialysis bag at t_w, the second subsection being devoted to the evolution of the measured microstructure during the ageing process of some samples, mainly skaken gels and regenerated gels.

4.1. Freshly prepared samples - $t_w = 0$ The scattering behavior obtained by SAXS with these sols and shaken gels freshly prepared are all qualitatively comparable [24]. As an illustration of that point, left part of Fig. 2 plots the scattered intensity I (normalized by Φ) as a function of the scattering vector q obtained by SAXS for samples D and E of Table 1 at $pH \sim 3$ and several values of I_{ion}. At large q's whatever I_{ion}, the intensity $I(q)$ scales as q^{-4} showing that on the local scale we probe in the experiment the surface of the NP's in their Porod regime [27]. On the contrary, at low q's, the $I(q)$ behavior largely depends on the value of I_{ion}. At the lowest ionic strength, $I(q)$ presents in both samples a maximum at q slightly above 0.01 Å^{-1} expressing that in these conditions the balance of interparticle interaction is repulsive in the dispersion. The gradual increase of ionic strength progressively distorts the shape of $I(q)$ at low q's in the two samples, up to obtain an increase by a factor 100 of the scattered intensity at the lowest q's with a $\sim q^{-2}$ behavior at intermediate q's. This $\sim q^{-2}$ behavior of the scattered intensity is the signature of a Reaction or a Diffusion Limited Cluster Aggregation of the NPs [33] expressing that in these conditions the balance of interparticle interaction is attractive in the dispersion. In between, the second coefficient of the virial of the osmotic pressure in the dispersion, which is positive when the balance of interparticle interaction is repulsive and negative when it is attractive, passes through zero at an intermediate I_{ion}, as in [13, 34]. In this "non-interacting" condition, the structure factor equals 1 whatever q. As $I_{nonInt}(q) \propto F(q)$, it allows for each sample the determination of the form factor $F(q)$ of the NPs and using

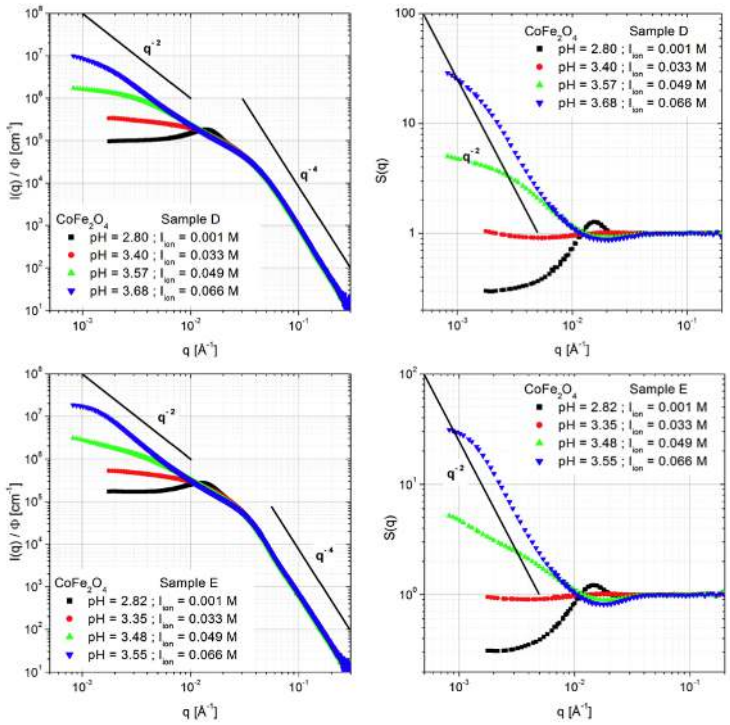

Figure 2: Freshly prepared samples - Scattered intensity I normalized by the volume fraction Φ (left part) and structure factor S (right part) as a function of the scattering vector q for Cobalt ferrite samples D (top curves) and E (bottom curves) from Table 1 at $pH \sim 3$ and various I_{ion}

Eq. (2) the determination of the structure factor $S(q)$ at any ionic strength I_{ion} and any pH.

The right part of Fig. 2 shows the $S(q)$ determinations associated to the intensities $I(q)$ of left part of Fig. 2. In both cases, the structure factor at the lowest ionic strength is repulsive, with an isothermal compressibility of the order of 0.3 and a marked maximum at the mean interparticle distance. On the contrary the plots at the two highest ionic strength corresponds to aggregated situations. Making in a first step the hypothesis that the formed clusters are not interacting, we can tentatively analyze the very low q's part of these curves in terms of a Guinier regime of clusters and extract their radius of gyration R_g and their number of aggregation N_{agg} (see Eq. 3). In the conditions of Fig. 2-right, the maximum N_{agg} value which is reached is of the order of a few 10 NPs.

Plotting the N_{agg}-dependence of R_g allows to determine the fractal dimension of the cluster. This is plotted for all the samples of Table 1 at $pH \sim 2$ in Fig. 3-left, which shows that on average R_g then scales as $\sim N_{agg}^{1/2}$. A similar result is found at $pH \sim 3$. This corresponds to loosy clusters with a fractal dimension of 2, consistent with the observation of $S(q) \propto q^{-2}$ in the intermediate regime of q's at the highest I_{ion} in Fig. 2-right. The strong dependence of N_{agg} on I_{ion} and pH is illustrated for sample A and D in Fig. 3-right . Note however that for the largest I_{ion} values, typically for N_{agg} larger than 100, the experimental system is a gel. It is doubtfull that in these conditions, where clusters are necessarily interconnected,

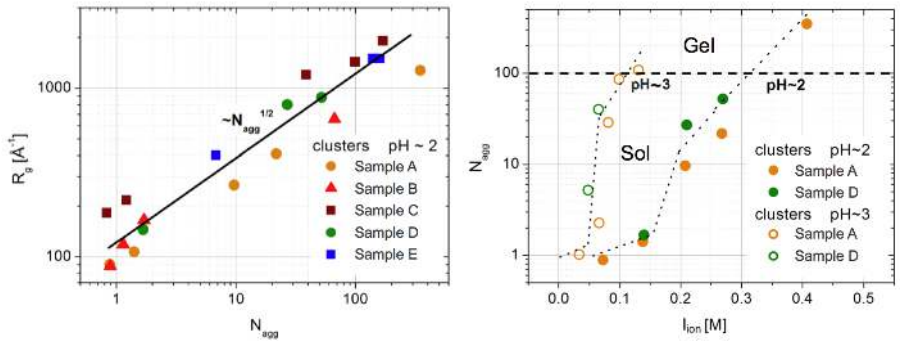

Figure 3: Characteristics of the clusters obtained in Guinier approximation : (left part) - R_g as function of N_{agg} at $pH \sim 2$ and various I_{ion} for all the probed samples; (right part) - I_{ion}-dependence of N_{agg} at $pH \sim 2$ and 3 for samples A and D of Table 1.

Guinier approximation still applies.

Fitting the low-q shape of $S(q)$ in the attractive regime with a Lorentzian

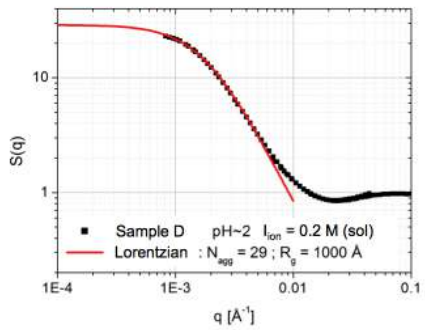

Figure 4: Adjustment of low-q shape of $S(q)$ by a Lorentzian in a sol of independent clusters (sample D of Table 1 at $pH \sim 2$ and $I_{ion} = 0.2$ mol/L)

is another tentative way to approach the characteristics of clusters with a fractal dimension of the order of 2. Fig. 4 presents an example of such a fit for sample D at $pH \sim 2$ and $I_{ion} = 0.2$ mol/L. In that case the obtained results $R_g = 10^3$ Å and $N_{agg} = 29$ are very close to those obtained with the Guinier method. On the contrary with a gel, such a fit by a Lorentzian is no more possible, expressing that in these conditions an inter-cluster interaction is also present.

4.2. Time evolution of the ageing samples - $t_w > 0$ As already said in part 2, the structure of these systems presents ageing properties which are macroscopically detectable as some of these samples clearly undergo a sol-gel transition in a time t_w which can typically vary from a fraction of second to 10^7 s depending on I_{ion} and pH [24]. As already said, the detailed dynamical study of this sol-gel transition is out of the scope of the present paper and will be presented elsewhere.

However we have to distinguish here between the time during which this first aggregation of the NPs occurs in the samples and the time necessary to regenerate shaken gels that were spontaneously formed previously.

Fig. 5-left shows the evolution of the SAXS intensity $I(q)$ for sample B at pH = 2.03 and I_{ion} = 0.13 mol/L. At $t_w = 0$, this freshly prepared sample presents only a slight aggregation, almost undetectable. However, two weeks after, at t_w = 16 days, the system presents clusters of $N_{agg} \sim 9$, as obtained by an adjustment of the low-q shape of $S(q)$ by a Lorentzian. After $t_w = 65$ days, the system is already a thixotropic gel, an adjustment by a Lorentzian of the low-q shape of $S(q)$ is no more possible.

As observed with several samples, regenerated gels do not present any long term ageing of their structure. Experiments performed on regenerated gels at t_w = 65 days with samples that are already gels at $t_w = 0$ show a quite similar $I(q)$ at the two ages [24]. SAXS measurements at low q's and resolved in time will be necessary to catch the structure evolution during the regeneration step of the gel structure.

The regenerated gels present a plateau (or a local maximum) of $I(q)$ at low

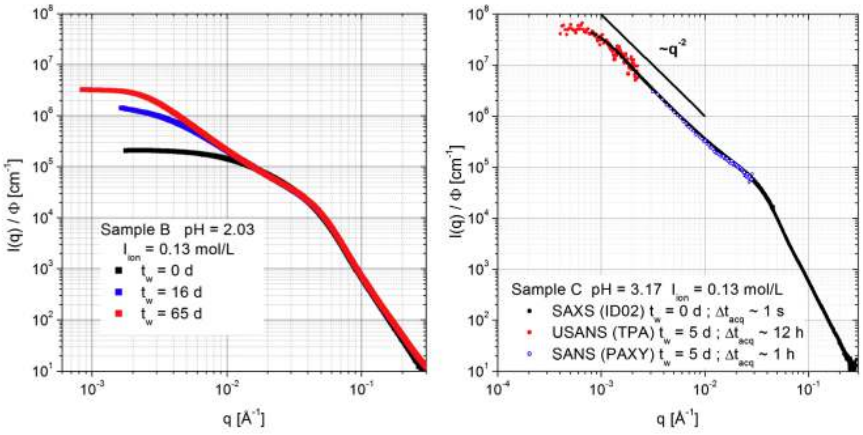

Figure 5: Small angle scattered intensity $I(q)/\Phi$ at different ages t_w: (left) - SAXS determinations of $I(q)$ for sample B at pH = 2.03 and I_{ion} = 0.13 mol/L at different ages t_w evolving from a sol of clusters towards a regenarated gel (from bottom to top t_w = 0, 16 days and 65 days); (right) - Comparison of SAXS and USANS determinations of $I(q)$ for sample C at pH = 3 and I_{ion} = 0.13 mol/L which is a regenerated gel in the experimental probing conditions.

q's, which cannot be identified with a Guinier regime of clusters as said before, and which has more probably to be associated with an inter-cluster interaction. However the gels based on the largest NP's of Table 1 (namely samples C and E) are not reaching this plateau in the q-range of the here-performed SAXS experiment ($q \geqslant 8\ 10^{-4}$Å^{-1}). A complementary probing by USANS at TPA in LLB-Saclay is thus performed. Right part of Fig. 5 compares, for sample C at pH = 3 and I_{ion} = 0.13 mol/L, SAXS and USANS results, together with the normalizing SANS measurements performed at PAXY (the neutron scattered intensities are here given in terms of X-ray contrast of the NPs). The various experiments with quite different acquisition times (see fig. 5-right) performed either at $t_w = 0$ or 5 days give consistent results, expressing that indeed the structure in this regenerated gel does

not evolve during the probed time scale. The low-q plateau (or local maximum) which is not reached in SAXS experiment is here clearly evidenced in the USANS experiment. Thus the two samples of Fig. 5 with different size distributions and pH have the same behavior, with just a shift in q and $I(q)$ of the breaking of slope, which occurs at lower q's and a higher intensity with larger NPs at larger pH.

The questions remaining open concerns the inter-cluster interaction during the ageing process and in the gel structure. Are we observing the begining of a plateau in the $I(q)$ spectra? Is it a local maximum? Can this autosimilarity breaking be associated to the characteristic size of clusters in attractive interaction as it is observed in [35, 36, 37]? Is the structure macroscopically homogeneous or not? The answer can only be given by a probing at even lower q's, by light scattering for example.

Conclusions In home-made aqueous acidic ferrofluids it is thus possible to monitor the average interparticle interaction from a global repulsion, leading to a homogeneous structure with clearly defined mean inter-particle distance and isothermal compressibility, to a global interparticle attraction, leading to sols of clusters and thixotropic gels. The sols of clusters present ageing properties that largely depend on the details of the electrostatic repulsion, through pH and ionic strength. The observed clusters have a rather loosy structure with a fractal dimension of the order of 2, as resulting from Diffusion or Reaction Limited Cluster Aggregation. At the first order, the present study does not show any structural dependence of the clusters and of the thixotropic gels on the ferrite material nor on the size of the NPs. A detailed dynamical study by magneto-birefringence, of the first NP aggregation process to form the clusters and ultimately the initial thixotropic gel is under progress.

Acknowledgements We thank M. Sztucki and T. Narayanan for their help during SAXS experiments at ID02 - ESRF and acknowledge the support of ESRF-Grenoble-France for the beamtime allocation. We also deeply thank S. Désert and A. Brulet, for the development and tuning of TPA spectrometer in LLB - Saclay and for the free access to TPA for the present tests. We are also very gratefull to D. Talbot for the synthesis of the nanoparticles and for the magnetic characterizations of the ferrofluids.

REFERENCES

1. R. Rosensweig. Ferrohydrodynamics. *Cambridge University Press*, Cambridge, 1985.
2. B. Berkovski Ed. Magnetic fluids and Applications Handbook. *Begell House Inc. Publ.*, N.Y., 1996.
3. S. Odenbach Ed. Magnetically controllable fluids and their applications. *Springer Verlag*, Berlin , 2010.
4. A. Elaissari. Colloidal Nanoparticles in Biotechnology. *John Wiley & sons, Inc.*, Hoboken, N.J., 2008.
5. C. Sanson, O. Diou, J. Thévenot, E. Ibarboure, A. Soum, A. Brulet, S. Miraux, E. Thiaidire, S. Tan, A. Brisson, V. Dupuis, O. Sandre, S. Lecommandoux. Doxorubicin loaded magnetic polymersomes : theranostic nanocarriers for MR Imaging and magneto-chemotherapy. *ACS Nano*, vol. 5 (2011), pp. 1122–1140.
6. G. Beaune, M. Levy, S. Neveu, F. Gazeau, C. Wilhelm, C. Ménager. Different localizations of hydrophobic magnetic nanoparticles within vesicles trigger their efficiency as magnetic nano-heaters. *Soft Matter*, vol. 7 (2011), pp. 6248–6254.

7. L.F. Shen, A. Stachowiak, S-E. K. Fateen, P. E. Laibinis, T.A. Hatton. Structure of alkanoic acid stabilized magnetic fluids. A small-angle neutron and light scattering analysis. *Langmuir*, vol. 17 (2001), pp. 288–299.

8. R. Itri, J. Depeyrot, F.A. Tourinho, M.H. Sousa. Nanoparticle chain-like formation in electrical double-layered magnetic fluids evidenced by small angle X-ray scattering. *Eur. Phys. J. E*, vol. 4 (2001), pp. 201–208.

9. V.L. Aksenov, M.V. Avdeev, M. Balasoiu, D. Bica, L. Rosta, Gy. Trk, L. Vekas. Aggregation in non-ionic water-based ferrofluids by small angle neutron scattering. *J. Magn. and Magn. Mat.*, vol. 258-259 (2003), pp. 452–455.

10. K. Butter, P.H.H. Bomans, P.M. Frederik, J. Vroege, A.P. Philipse. Direct observation of dipolar chains in iron ferrofluids by cryogenic electron microscopy. *Nature materials*, vol. 2 (2003), pp. 88–91.

11. L.M. Pop, S. Odenbach, A. Wiedenmann, N. Matoussevitch, H. Bonnemann. Microsctructure and rheology of ferrofluids. *J. Magn. and Magn. Mat.*, vol. 289 (2005), pp. 303–306.

12. A.F. Pshenichnikov, A.A. Fedorenko. Chain-like aggregates in magnetic fluids. *J. Magn. and Magn. Mat.*, vol. 292 (2005), pp. 332–344.

13. F. Cousin, E. Dubois, V. Cabuil. Tuning the interactions of a magnetic colloidal dispersion. *Phys.Rev. E*, vol. 68 (2003), 021405 pp. 1–9.

14. G. Mériguet, F. Cousin, E. Dubois, F. Boué, A. Cebers, B. Farago, R. Perzynski. What tunes the structural anisotropy of magnetic fluids under a magnetic field ? *J.Phys.Chem. B*, vol. 110 (2006), pp. 4378–4386.

15. G. Mériguet, E. Wandersman, E. Dubois, A. Cebers, J. de Andrade Gomes, G. Demouchy, J. Depeyrot, A. Robert, R. Perzynski. Magnetic fluids with tunable interparticle interaction : monitoring the under-field local structure. *Magnetohydrodynamics*, vol. 48 (2012), pp. 415–425.

16. E. Hasmonay, A. Bee, J.C. Bacri, R. Perzynski. *pH* effect on an ionic ferrofluid : evidence of a thixotropic magnetic phase. *J.Phys.Chem. B*, vol. 103 (1999), pp. 6421–6428.

17. R. Massart. Preparation of aqueous magnetic liquids in alkaline and acidic media. *IEEE Trans Mag Magn*, vol. 17 (1981), pp. 1247–1248.

18. A. Bee, R. Massart, S. Neveu. Synthesis of very fine magnetic particles. *J. Magn. and Magn. Mat.*, vol. 149 (1995), pp. 6–9.

19. R. Massart, E. Dubois, V. Cabuil, E. Hasmonay. Preparation and properties of monodispersed magnetic fluids. *J. Magn. and Magn. Mat.*, vol. 149 (1995), pp. 1–5.

20. A.F.C. Campos, F.A. Tourinho, G.J. da Silva, M.C.F.L. Lara, J. Depeyrot. Nanoparticles superficial density of charge in electric double layered magnetic fluids : a conductimetric and potentiometric approach. *Eur.Phys.J.*, vol. 6 (2001), pp. 29–35.

21. F.A. Tourinho, A.F.C. Campos, R. Aquino, M.C.F.L. Lara, G.J. da Silva, J. Depeyrot. Surface charge density determination in electric double layered Magnetic Fluids. *Braz.J.Phys.*, vol. 32 (2002), pp. 501–508.

22. I.T. Lucas, S. Durand-Vidal, E. Dubois, J. Chevalet, P. Turq. Surface charge density of maghemite nanoparticles : role of electrostatics in the proton exchange. *J.Phys.Chem. C*, vol. 111 (2007), pp. 18568 –18576.

23. V.A. Parsegian, N. Fuller, R.P. Rand. Measured work of deformation and repulsion of lecithin bilayers. *Proc.Nat.Acad.Sci.*, vol. 76 (1979), pp. 2750-2754.

24. B. Frka-Petesic Aggregates of self-assembled magnetic particles *Thèse de l'Université Pierre et Marie Curie - Paris 6, France*, (2010)

25. A. Ponton, A. Bee, E. Hasmonay, R. Perzynski, J.-C. Bacri. Dynamic probing of thixotropic magnetic gels. *J. Magn. and Magn. Mat.*, vol. 252 (2002), pp. 232–234.

26. A. Ponton, A. Bee, D. Talbot, R. Perzynski. Regeneration of thixotropic magnetic gels studied by mechanical spectroscopy: the effect of the pH. *J.Phys.Cond.Matter*, vol. 17 (2005), pp. 821–836.

27. M.V. Avdeev, E. Dubois, G. Mériguet, E. Wandersman, V.M. Garamus, A.V. Feoktystov, R. Perzynski. Small-angle neutron scattering analysis of a water-based magnetic fluid with charged stabilization : contrast variation and scattering of polarized neutrons. *J.Appl.Cryst.*, vol. 42 (2009), pp. 1009–1019.

28. E. Dubois, V. Cabuil, F. Boué, R. Perzynski. Structural analogy between aqueous and oily magnetic fluids. *J.Chem.Phys.*, vol. 111 (1999), pp. 7147–7160.

29. F. Gazeau, F. Boué, E. Dubois, R. Perzynski. Static and quasi-elastic small angle neutron scattering on biocompatible ionic ferrofluids : magnetic and hydrodynamic interactions. *J.Phys.: Cond.Matt.*, vol. 15 (2003), pp. S1305–S1334.

30. S. Lecommandoux, O. Sandre, F. Chécot, J. Rodriguez-Hernandez, R. Perzynski. Magnetic nanocomposite micelles and vesicles. *Adv.Mater.*, vol. 17 (2003), pp. 712–718.

31. S. Rivière, C. Wilhelm, F. Cousin, V. Dupuis, F. Gazeau, R. Perzynski. Internal structure of magnetic endosomes. *Eur.Phys.J.E*, vol. 22 (2007), pp. 1–10.

32. J. Fresnais, J.-F. Berret, L. Qi, J.-P. Chapel, J.-C. Castaing, O. Sandre, B. Frka-Petesic, R. Perzynski, J. Oberdisse, F. Cousin. Universal scattering behavior of coassembled nanoparticle-polymer clusters. *Phys.Rev.E*, vol. 78 (2008), 040401(R) pp. 1–4.

33. M.Y. Lin, E. Dubois, H.M. Lindsay, D.A. Weitz, R.C. Ball, R. Klein, P. Meakin. Universal reaction-limited colloid aggregation. *Phys.Rev. A*, vol. 41 (1990), pp. 2005–2020.

34. E. Dubois, R. Perzynski, F. Boué, V. Cabuil. Liquid-Gas transitions in charged colloidal dispersions : Small-Angle Neutron Scattering coupled with phase diagrams of magnetic fluids. *Langmuir*, vol. 16 (2000), pp. 5617–5625.

35. N. Jouault, P. Vallat, F. Dalmas, S. Said, J. Jestin, F. Boué. Well-dispersed fractal aggregates as filler in polymer-silica nanocomposites : long-range effects in rheology. *Macromolecules*, vol. 42 (2009), pp. 2031–2040.

36. A.S. Robbes, J. Jestin, F. Meneau, F. Dalmas, O. Sandre, J. Perez, F. Boué, F. Cousin. Homogeneous dispersion of magnetic nanoparticles aggregates in a PS nanocomposite: highly reproductible hierarchical structure tuned by nanoparticles sizes. *Macromolecules*, vol. 43 (2010), pp. 5785–5796.

37. H. Wu, J.J. Xie, M. Morbidelli. Kinetics of colloidal gelation and scaling of the gelation point. *Soft Matter*, vol. 9 (2013), pp. 4437–4443.